ESR, ENDOR AND TRIPLE RESONANCE STUDIES OF THE PRIMARY DONOR RADICAL CATION $P_{960}^{+\cdot}$ IN THE PHOTOSYNTHETIC BACTERIUM *RHODOPSEUDOMONAS VIRIDIS*

F. LENDZIAN [a], W. LUBITZ [b], H. SCHEER [c], A.J. HOFF [d], M. PLATO [a], E. TRÄNKLE [e] and K. MÖBIUS [a]

[a] *Institut für Molekülphysik, Freie Universität Berlin, D-1000 Berlin 33, Germany*
[b] *Institut für Organische Chemie, Freie Universität Berlin, D-1000 Berlin 33, Germany*
[c] *Institut für Botanik, Universität München, D-8000 Munich, Federal Republic of Germany*
[d] *Department of Biophysics, Huygens Laboratory of the State University, 2300 RA Leyden, The Netherlands*
[e] *Institut für Theorie der Elementarteilchen, Freie Universität Berlin, D-1000 Berlin 33, Germany*

Received 5 May 1988

The light-induced radical cation of the primary electron donor $P_{960}^{+\cdot}$ in photosynthetic reaction centers from *Rhodopseudomonas viridis* has been investigated by ESR, ENDOR and TRIPLE techniques. Both the comparison with the cation radical of monomeric bacteriochlorophyll **b** (BChl **b**) and with molecular-orbital calculations performed on $P_{960}^{+\cdot}$ using the results of an X-ray structure analysis, consistently show an asymmetric distribution of the unpaired electron over the two BChl **b** molecules which constitute $P_{960}^{+\cdot}$. The possible relevance of this result for the primary electron transfer step in the reaction center is briefly discussed.

1. Introduction

The primary processes in bacterial reaction centers (RCs) involve light excitation of the primary donor P followed by fast electron transfer reactions [1–3]. The participating molecules are bacteriochlorophylls (BChl), bacteriopheophytins and quinones, which are all imbedded in the RC protein complex. The RC of the photosynthetic bacterium *Rhodopseudomonas* (*Rps.*) *viridis* has recently been crystallized [4] and its structure has been determined by X-ray diffraction [5–7]. Apart from the *spatial* structure a knowledge of the *electronic* structure of the pigment molecules – including their environment – is of importance for an understanding of the functional properties of the RC. For paramagnetic states this information can be obtained from ESR and electron–nuclear multiple resonance experiments [8,9]. Based on ESR techniques Norris et al. [10] proposed in 1971 for bacteria containing bacteriochlorophyll **a** that a BChl **a** dimer forms the primary electron donor (P_{870}) in the RC. This was concluded from a $1/\sqrt{2}$ line narrowing of the ESR spectrum and a reduction of the ENDOR (electron–nuclear double resonance) splittings by a factor of two at low temperatures when $P_{870}^{+\cdot}$ and monomeric BChl $\mathbf{a}^{+\cdot}$ were compared [11,12]. These experimental findings have been interpreted as arising from an *equal* sharing of the unpaired electron between two BChl **a** molecules. Later ENDOR investigations of RCs in liquid solution supported the model of a symmetric dimeric supermolecule for $P_{870}^{+\cdot}$ [13–16].

Although the X-ray structure analysis of the RC of BChl **b** (fig. 1) containing bacterium *Rps. viridis* shows the existence of a BChl **b** dimer [5–7], the cation of the primary donor, $P_{960}^{+\cdot}$ does not display the $1/\sqrt{2}$ narrowing of the ESR spectrum nor the 50% reduction of the solid state ENDOR splittings when compared with BChl $\mathbf{b}^{+\cdot}$ [17].

In this paper we present liquid solution ENDOR and TRIPLE (electron–nuclear–nuclear triple resonance) experiments on $P_{960}^{+\cdot}$ in RCs of *Rps. viridis* at room temperature and give a comparison with corresponding results for BChl $\mathbf{b}^{+\cdot}$ [18]. Our results show an asymmetrical distribution of the unpaired electron over the two BChl **b** molecules constituting $P_{960}^{+\cdot}$. This finding is in agreement with molecular orbital (MO) calculations of the RHF INDO/SP type

0 009-2614/88/$ 03.50

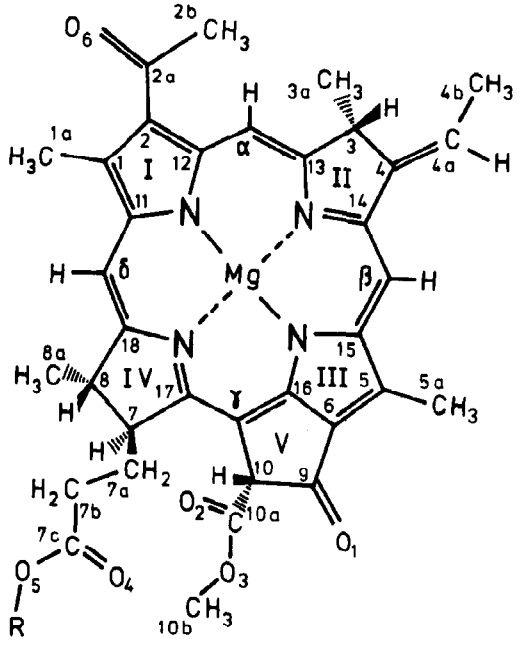

Fig. 1. Molecular structure and numbering scheme of bacteriochlorophyll **b** (BChl **b**). R = phytyl ($C_{20}H_{39}$) in *Rps. viridis*. The 4, 4a double bond is hydrogenated in BChl **a**.

[19] performed on P_{960}^{+} using atomic coordinates from the X-ray structure analysis [5–7]. Preliminary reports of this work have already been given [20,21].

2. Materials and methods

Rhodopseudomonas viridis was grown in 1 ℓ culture bottles in medium No. 27 (Deutsche Sammlung von Mikroorganismen). The following changes were made for the selective deuteration: The medium was made up in deuterium oxide (≥ 99% D_2O), all phosphates were exchanged prior to use by dissolving them four times in D_2O and subsequent lyophilizations; the same procedure was used for trace element solution. Ethanol was omitted, yeast extract was replaced by yeast concentrate (Sigma, 0.5 g/ℓ), and the medium was supplemented with *p*-aminobenzoic acid (1 mg/ℓ). Succinate was used in the protic form. Work-up was done in protic media throughout for both H- and D-RCs.

Chromatophores and crude reaction centers (Munich laboratory) were prepared by minor modification of the method of Jolchine and Reiss-Housson [22]. Extraction of the LDAO- (lauryldimethylamine oxide) treated membrane ($OD_{1020} = 50$ cm^{-1}) with low LDAO concentrations (1.5%) was repeated once or twice if necessary to remove the RCs. Crude reaction centers were purified on DEAE- (diethylaminoethyl) cellulose. For deuterated RCs exchange of LDAO against Triton X-100 (Roth) was carried out by a modification of the method of Pachence et al. [23] to increase the RC stability. The sample was loaded on a DEAE-cellulose column equilibrated against tris-buffer (20 mM, *pH* 7.5) containing 1% Triton X-100. It was subsequently washed with this buffer, with the same buffer containing sodium dithionite, and again with the starting buffer. The RCs were removed with 200 mM NaCl in this buffer and concentrated by membrane filtration (BM100, Berghof). Since the D-RCs are more labile than the H-RCs the concentration was carried out in four steps. In each single step, the concentration was not increased by more than fivefold. The solution was then treated with amberlite XAD-2 (Serva, 0.2 g/ml) for 1 h on ice to remove excess detergent (Triton X-100) [24], the resin removed by centrifugation, and the procedure continued to a final concentration of ≈200 μM.

H-RCs were prepared by the same method with LDAO without exchange of detergent and one-step concentration to the desired value (≈400 μM). An alternative method (Leyden laboratory) essentially followed the procedure described in ref. [25] using a treatment with high LDAO concentration (6%) followed by sucrose gradient centrifugation and final purification on DEAE.

Bacteriochlorophyll **b** was extracted from bacteria and purified as described in ref. [26]. The isotope substitution pattern of the partially deuterated BChl **b** (D_2O/succinate-*h*) was determined by ^1H NMR spectroscopy at 360 MHz in pyridine-*d*. Details of the assignments are published elsewhere [27].

P_{960}^{+} has been generated by in situ illumination with a 100 W tungsten lamp in the range 450–1000 nm or, alternatively, by oxidation with $K_3Fe(CN)_6$ (0.05 M) [17].

A detailed description of the laboratory-built ENDOR/TRIPLE spectrometer including the probe

head for in situ illumination has been given elsewhere [8,28].

The s-spin densities and total energies for geometry optimization of BChl $\mathbf{b}^{+\cdot}$ [118] were calculated by a restricted Hartree–Fock procedure for doublet states (the "half-electron method" of Dewar [29]) using the INDO approximation and parametrization by Pople and Beveridge [30] and a subsequent perturbation treatment of spin polarization effects (RHF INDO/SP method). The details of this procedure are presented in ref. [19]. We have recently developed a new SP version which has full rotational invariance for s-spin densities and gives improved results [31]. Calculations on $P_{960}^{+\cdot}$ in RCs of *Rps. viridis* were performed on the structure given by the X-ray data (2.9 Å resolution, $R=0.231$) [7] with hydrogen atoms attached by standard rules [30]. All calculations were done on the CRAY X-MP/24 of the Konrad-Zuse-Rechenzentrum at Berlin.

A computer deconvolution of the special TRIPLE spectra has been performed to separate strongly overlapping lines and to determine their relative intensities. As line shape function for a single line we chose a frequency modulated Lorentzian line which gave a good fit to single line spectra. A sum of derivatives of n single distribution functions together with a base-line shift was adjusted to the ENDOR spectra by a least-squares fit. The positions and the widths of the lines were determined using the iterative minimization algorithm SIMPLEX whereas the area parameters and the base-line shift were calculated by solving a system of linear algebraic equations obtained from the partial derivatives of the sum of the least-squares. The frequency modulation parameter was taken from the experimental spectra.

3. Results and discussion

The ESR linewidths of BChl $\mathbf{b}^{+\cdot}$ and $P_{960}^{+\cdot}$ in liquid solution are 12.6 ± 0.2 [18] and 11.6 ± 0.2 G, respectively. In frozen solution, where broadening due to anisotropic hfs and g-values occurs, the corresponding values are 13.5 ± 0.2 [18] and 11.8 ± 0.2 G [17]. The line-narrowing factor is thus 0.92 in liquid and 0.87 in frozen solution. This small difference in the linewidths of the monomeric (in vitro) and dimeric (in vivo) cation radicals is in remarkable contrast to the results for BChl **a** containing bacteria *Rhodobacter sphaeroides* and *Rhodospirillum rubrum*, where a $1/\sqrt{2}=0.71$ line narrowing is observed as compared with monomeric BChl $\mathbf{a}^{+\cdot}$. for

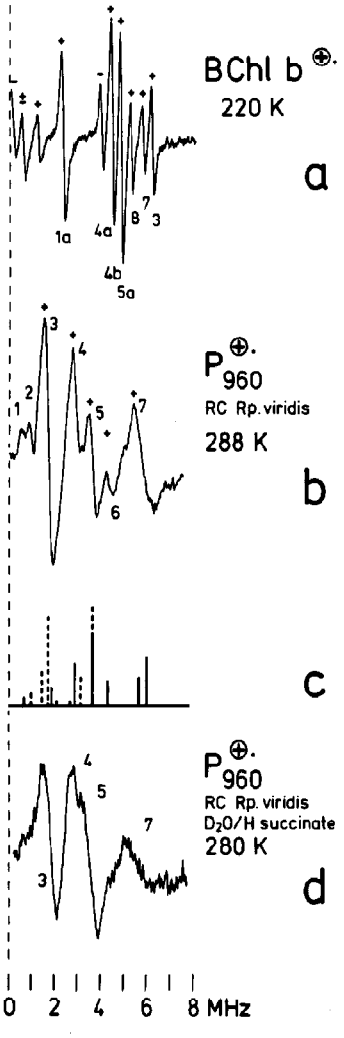

Fig. 2. Special TRIPLE resonance spectra of (a) BChl $\mathbf{b}^{+\cdot}$ in CH_2Cl_2/CH_3OH (6 : 1) at $T=220$ K, microwave power 80 mW, rf power 200 W [18]. (b) $P_{960}^{+\cdot}$ in illuminated RCs of *Rps. viridis* (see text), $T=288$ K, microwave power 60 mW, rf power 200 W. Sign determination by general TRIPLE resonance [9]. (c) Spectral components and relative amplitudes (stick diagram) as obtained from computer deconvolution (see text). Note that the ENDOR amplitudes do not reliably reflect the number of contributing nuclei due to their drastically different relaxation behaviour, particularly in this slowly tumbling protein (rotational correlation time $\tau_R \geq 50$ ns). The full and dotted lines correspond to the L and M dimer halves, respectively (assignment C, table 2). (d) Selectively deuterated $P_{960}^{+\cdot}$ (mainly methyl groups carry protons, see text). Conditions as in (b).

the latter case, this has been interpreted as being due to an equal sharing of the unpaired electron between the two BChl **a** dimer halves [10–16].

Figs. 2a and 2b show a comparison of the liquid solution special TRIPLE [9] spectra of BChl $\mathbf{b}^{+\cdot}$ and $P_{960}^{+\cdot}$. In this experiment two rf-frequency sidebands are swept symmetrically about the proton nuclear Zeeman frequency. Lines in the spectrum therefore appear at frequencies which correspond to one half of the respective hfcs [9].

Taking line broadening effects into account, spectrum b closely resembles the features of spectrum a, except for a small shift of the lines towards lower frequencies. For all observed lines this shift is much less than a factor of two. Instead, an average frequency reduction factor of about 1.3 can be obtained for lines 3 to 7 of fig. 2b. Such a phenomenological comparison of spectral features can, however, be misleading and the results obtained may be questionable. A reliable interpretation can only be obtained when ob-

Table 1
Experimental and calculated hfcs of BChl $\mathbf{b}^{+\cdot}$ and $P_{960}^{+\cdot}$ (MHz)

BChl $\mathbf{b}^{+\cdot}$			$P_{960}^{+\cdot}$					
			measured		calculated [b]			
exp. [a]	calc. [b]	pos. [c]	exp [d] (n) [g]	comp. [e]	L [f]	pos. [c]	M [f]	pos. [c]
0.40	−0.02, −0.15	2b, 3a	+1.4 (1)	1.33	+1.36	β	+0.75	1a
	−0.23, −0.38	8a, 7a					+0.88	β
							−1.56	10
1.20	+2.46, −2.56	δ, 10	+2.0 (2)	1.95	+1.91, −1.95	α, 10	+1.56	δ
+2.50	+2.59, +3.16	β, α			+2.17	δ	+1.27	α
+4.70	+4.57	1a	+3.43 (3)	2.82			−1.79	4a
−8.02	−4.70	4a		3.35			+2.16	5a
				3.72			+2.79	4b
+8.95	+7.59	4b		4.12			+5.85	7
+9.70	+9.24	5a	+6.0 (4)	5.25	−3.52	4a		
+10.55	+11.42	8		5.75	+4.59	1a		
				6.20	+5.17	5a	+6.59	3
+11.60	+11.80	7	+7.2 (5)	7.21	+5.63	4b	+8.32	8
+12.45	+14.94	3	+8.5 (6)	8.57	+12.70	3		
			+11.5 (7)	11.25	+12.85	8		
				11.97	+17.12	7		

[a] Oxidized with $ZnTPP^{+}ClO_4^{-}$ in CH_2Cl_2/CH_3OH solution (6 : 1) at T=220 K [18]). Specific assignments within the groups of β-protons (positions 8, 7, 3) and CH_3 protons (1a, 4b, 5a) rely on comparison with the calculation and on experimental assignments obtained for BChl $\mathbf{a}^{+\cdot}$ [32]. Signs from general TRIPLE; not determined if omitted.

[b] Calculated with RHF INDO/SP, see refs. [19,31].

[c] See molecular structure of BChl **b**, fig. 1. Small hfcs of BChl $\mathbf{b}^{+\cdot}$ have been reassigned as compared with ref. [18]. For $P_{960}^{+\cdot}$ lines 3, 4 and 5 were shown to contain methyl protons by selective deuteration (see fig. 2d); further assignments from comparison with BChl $\mathbf{b}^{+\cdot}$ and with the RHF INDO/SP calculations (see tabel 2, assignment B).

[d] From spectrum in fig. 2b; signs determined by general TRIPLE resonance. Note that the "effective" signs measured for a line containing several spectral components (line numbers n=3, 4 and 7) need not be the same for each component.

[e] Components of the experimental spectrum as obtained by computer deconvolution (see text). The single components (line numbers 1 and 2) could not be further resolved but are expected to still contain several subcomponents.

[f] L and M are the BChl **b** dimer halves bound to the L an M protein subunits (see refs. [5–7]). The calculated hfcs on the L and M halves are assigned either individually or in groups (brackets) to the various spectral components.

[g] n=line number used in fig. 2b.

served lines can be individually assigned to molecular positions.

For monomeric BChl $\mathbf{b}^{+\cdot}$ an assignment could be achieved for the largest seven proton hyperfine couplings (hfcs) by sign determination using general TRIPLE resonance [9], by comparison with BChl $\mathbf{a}^{+\cdot}$ [18,28,32] and by the aid of RHF-INDO/SP calculations [18]. The result is given in table 1.

For $P_{960}^{+\cdot}$ the situation is much more difficult. For an asymmetrical dimer twice the number of lines is expected in the spectrum as compared with BChl $\mathbf{b}^{+\cdot}$. Owing to reduced hfcs these lines appear in a smaller frequency range. Moreover, because of the slow tumbling of the large protein in the aqueous solution (a correlation time of > 50 ns can be estimated [13]), the observed ENDOR linewidths are larger by a factor of 3–4 than those found for BChl $\mathbf{b}^{+\cdot}$. The result is a poorly resolved spectrum of strongly overlapping lines. We have attempted to overcome this problem by computer deconvolution of the spectrum from fig. 2b (see above). The best fit of the experimental spectrum was obtained when the intense lines 3, 4 and 5 (fig. 2b) were assumed to consist of several components. The result is shown in form of a stick diagram in fig. 2c. Table 1 comprises the hfcs obtained both from the computer deconvolution (comp.) and directly from the zero crossing in spectrum 2b (exp.).

The results differ from earlier ENDOR data measured for $P_{960}^{+\cdot}$ in frozen solution [17]. Our hfcs obtained from frozen solution spectra (fig. 3a) also disagree with those in ref. [17]. However, except for a considerable broadening of the lines, our liquid and frozen solution spectra (figs. 2b and 3a) are consistent. Furthermore, we obtained identical spectra for both illuminated and chemically oxidized samples. Moreover, we studied several RC preparations of *Rps. viridis* isolated in two different laboratories (HS, Munich, and AJH, Leyden, see section 2) and always found the same spectra. Our ESR spectra, however, agree with the earlier data [17].

Assignment of the observed hfcs of $P_{960}^{+\cdot}$ to molecular positions in the BChl **b** moieties could in part be obtained by comparison with spectra in frozen solutions (fig. 3) and by selective biosynthetic deuteration (fig. 2d). In the latter case the bacteria are grown in D_2O and fed with succinate-*h*. The resulting isotopic constitution of BChl **b** is expected to be

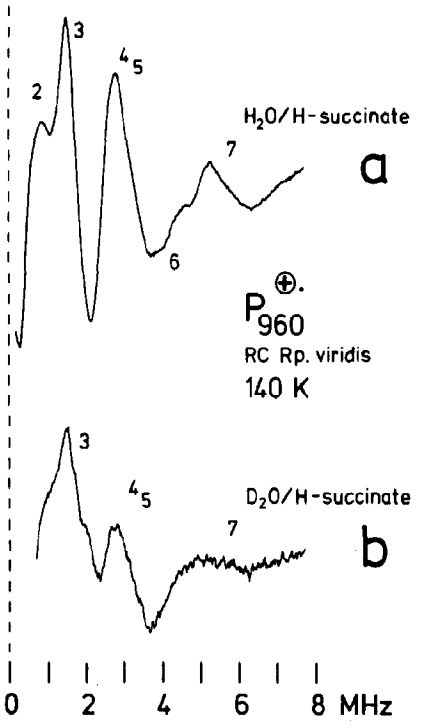

Fig. 3. Special TRIPLE resonance spectra of $P_{960}^{+\cdot}$ in illuminated frozen RC solutions of *Rps. viridis*, microwave power 12 mW, rf power 150 W. (a) Fully protonated, (b) selectively deuterated (mainly methyl groups carry protons, see text).

similar to that in the BChl **a** containing bacteria (*Rb. sphaeroides* and *Rs. rubrum*). In these organisms only the methyl groups of BChl **a** carry protons (about 40%). The methine positions (α, β, δ, fig. 1) and the positions 3, 4, 7, 8 are more than 90% deuterated [14,15,33,34]. This labelling pattern is also observed in *Rps. viridis* [27]. Due to the slow growth in D_2O, however, the differences between hydrogens derived from succinate-*h* and from D_2O are less pronounced: carbon positions 1a, 5a and 4b (relevant methyl groups) carry $\approx 50\%$ deuterons on the average, position 4a $\approx 70\%$ and the methine positions (α, β, δ) $\approx 85\%$; the β-protons attached to carbon 3, 7, and 8 are, on the average, $\geqslant 70\%$ deuterated. These values are sufficiently different to assign the lines 3, 4 and 5 to the methyl protons (1a, 4b, 5a) in the ENDOR spectra (figs. 2b and 2d). This finding is also consistent with spectra of $P_{960}^{+\cdot}$ obtained in frozen solution (fig. 3), where only protons of freely rotating methyl groups give rise to intense lines,

of other β-protons and α-protons are considerably broadened [12,35]. Any further assignment of the hfcs of $P_{960}^{+\cdot}$ has to rely on comparison with monomeric BChl $\mathbf{b}^{+\cdot}$ or on MO calculations for $P_{960}^{+\cdot}$. Table 1 comprises the results of our RHF INDO/SP calculations on BChl $\mathbf{b}^{+\cdot}$ [18] and on $P_{960}^{+\cdot}$ [31].

A comparison of the experimental and calculated hfcs for BChl $\mathbf{b}^{+\cdot}$ gives an overall good agreement. The calculated values for the β-protons (positions 3, 7, 8) are about 10% too large; the values for the methyl protons (positions 1a, 5a, 4b) are about 8% too small. The calculated largest α-H hfc (position 4a) is, however, 40% too small. These deviations obtained for BChl $\mathbf{b}^{+\cdot}$ may be inherent in the MO calculation procedure and/or caused by uncertainties of the molecular structure, and should be taken into account when experimental and theoretical results for $P_{960}^{+\cdot}$ are compared.

The most striking result of the calculations performed on $P_{960}^{+\cdot}$ is the unequal distribution of the unpaired electron over the two BChl **b** molecules [21,31]. The ratio of the sums of the respective s- and p-spin densities is 0.74 : 0.26 in favor of the BChl **b** molecule in the dimer bound to the L-branch [5–7]. The agreement between the experimental and theoretical hfcs depends, of course, very much on the chosen assignment of experimental hfcs to molecular positions. A crucial point for any assignment is the simulation of the observed ESR spectrum of $P_{960}^{+\cdot}$. There may be several different assignments which fit the unresolved ESR spectrum of $P_{960}^{+\cdot}$ (fig. 4) equally well within experimental error. However, any assignment which fails to reproduce the ESR spectrum can definitely be discarded.

Three different assignments for $P_{960}^{+\cdot}$ are given in table 2, which are all consistent with the results of the selective deuteration (figs. 2 and 3):

Assignment A completely ignores the results of the RHF-INDO/SP calculations on $P_{960}^{+\cdot}$. Instead it relies on a symmetric dimer model and on a comparison with BChl $\mathbf{b}^{+\cdot}$. The obtained simulated ESR spectrum is much broader than the observed one (fig. 4A). This discrepancy persists even when only one proton (per BChl **b** molecule) is assigned to the largest experimental hfc. The experimental spectrum can only be matched when, in addition, two methyl groups (six protons) are removed from line 5 (hfc: 7.2 MHz) and assigned to line 3 (hfc: 3.4 MHz),

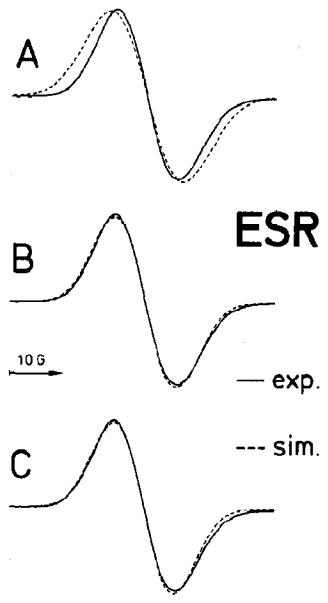

Fig. 4. Experimental and simulated ESR spectra of $P_{960}^{+\cdot}$ for the assignments A, B and C given in table 2. The ^{14}N hfcs of $P_{960}^{+\cdot}$ (not measured) were assumed to be half of the respective monomer BChl $\mathbf{b}^{+\cdot}$ values [18].

which is, however, in contradiction to the result of the selective deuteration. Another possibility for reducing the width of the simulated ESR spectrum of $P_{960}^{+\cdot}$ is the assumption of different β-proton hfcs at positions 3, 7, 8 (fig. 1) for the two BChl **b** halves of $P_{960}^{+\cdot}$. Since the hfcs of β-protons depend strongly on the dihedral angle θ between the C_α, C_β, H_β plane, such a situation might be met for different twist angles of the saturated rings II and IV in the two BChl **b** molecules [17] even though the two π carbon skeletons might be equivalent. When in case A (table 2) only one proton is assigned to each of the two lines 6 and 7 and the other four β-protons of positions 3, 7, 8 in the BChl **b** dimer are assigned to line 3, the simulated ESR spectrum is indeed in accordance with the observed one. There are, however, two arguments against such an assignment: (i) The factor 3 in the difference between the β-proton hfcs requires, for constant α-carbon spin densities, an estimated difference in the twist angles of rings II and/or IV of about 30°, which seems very unlikely [32]. (ii) For a symmetric dimer model the average hfc reduction factor, when comparing monomeric BChl $\mathbf{b}^{+\cdot}$ with $P_{960}^{+\cdot}$, should be 2. In the symmetric assignment A the

Table 2
Experimental hfcs (MHz) and assignments for $P_{960}^{+\cdot}$

hfc (MHz)		Assignment [g]				
exp. [a] (n) [f]	comp. [b]	A	B		C	
		pos. [c] (N) [d]	L [e]	M [e]	L [e]	M [e]
			pos. (N)	pos. (N)	pos. (N)	pos. (N)
+1.4 (1)	1.33	α, β, δ (6)	β (1)	1a, 10, β (5)	β (1)	1a, 10, β (5)
+2.0 (2)	1.95	10 (2)	δ, α, 10 (3)	δ, α (2)	δ, α, 10 (3)	δ, α (2)
+3.4(3)	2.82	1a (6)		4a (1)	1a (3)	5a (3)
	3.35			5a (3)		4a (3)
	3.72			4b (3)		
	4.12			7 (1)		4a (1)
+6.0 (4)	5.25	4a (2)	4a (1)		4a (1)	
	5.75	4b (6)	1a (3)		4b (3)	
	6.20		5a (3)	3 (1)		3, 7 (2)
+7.2 (5)	7.21	5a (6)	4b (3)	8 (1)	5a (3)	8 (1)
+8.5 (6)	8.57	3 (2)	3 (1)		3 (1)	
+11.5 (7)	11.25	8 (2)	8 (1)		8 (1)	
	11.97	7 (2)	7 (1)		7 (1)	

[a] From RC solutions of *Rps. viridis*, illuminated in situ at $T=288$ K.
[b] Components obtained by computer deconvolution (see text and table 1).
[c] For positions see molecular structure of BChl **b** (fig. 1).
[d] N=number of contributing protons.
[e] L and M are the BChl **b** dimer halves bound to the L and M protein subunits, respectively (see refs. [5–7]).
[f] n=line number used in fig. 2b.
[g] For assignments A to C see text. The assignment of the larger groups of hfcs to the L-half of the dimer is based on our MO calculations (see table 1).

average reduction factor of the methyl hfcs (positions 1a, 4b, 5a) is only 1.4. Thus, we conclude that a symmetric dimer is not consistent with the experimental results.

Assignment B relies mainly on the RHF INDO/SP calculations on $P_{960}^{+\cdot}$ performed on the X-ray data [7] given in table 1. It ignores, however, the relative intensities of the ENDOR/TRIPLE lines obtained from the deconvolution of the spectra. Although under favorable relaxation conditions special TRIPLE line intensities do reflect the number of contributing nuclei [8,9], these conditions might possibly not be met here, because of the slow tumbling of the protein in the liquid solution. According to the RHF INDO/SP calculation three methyl groups (1a, 5a, 4b) of the L dimer half are assigned to the spectral components at 5.75, 6.20 and 7.21 MHz, whereas the corresponding three groups of the M dimer half are assigned to the smaller hfcs 1.33, 3.35 and 3.72 MHz. The simulated ESR spectrum for this assignment agrees with the observed one (fig. 4). The obtained L/M ratio of the sum of the large hfcs at positions 1a, 4a, 4b, 5a, 3, 7 and 8 is 0.66/0.34, which is close to the result of the calculations (0.68/0.32) for these positions.

Assignment C partly takes into account the relative intensities of the spectral components as obtained from the deconvolution. It further relies to a certain extent on an analogy with the spectrum of BChl $\mathbf{b}^{+\cdot}$ (fig. 2a): The ratio of the methyl hfcs 5a and 1a is close to 2 in both dimer halves (L and M, respectively) and the three β-hfcs at positions 3, 7 and 8 have comparable magnitudes within one molecule, as is the case for monomeric BChl $\mathbf{b}^{+\cdot}$ (see table 1). The obtained ESR simulation for this assignment is also in accordance with the observed ESR

spectrum (fig. 4C). The L/M ratio of the large hfcs (1a, 4a, 4b, 5a, 3, 7 and 8) is 0.63/0.37. The calculated value for these positions is 0.68/0.32 (see table 1).

Although it is not possible to assign all proton hfcs individually to molecular positions in $P_{960}^{+\cdot}$ the general result of this work is an unequal distribution of the unpaired electron over the two BChl **b** molecules constituting $P_{960}^{+\cdot}$. The obtained spin density ratio in the L and M dimer halves is also in fair quantitative agreement with the results of our RHF INDO/SP calculations [21,31]. As will be shown in a forthcoming paper, the origin of the observed asymmetry in the spin density distribution of $P_{960}^{+\cdot}$ is a slight deviation of the dimer from exact C_2 symmetry and an additional asymmetric charge distribution of the surrounding polar amino acid residues [31]. Recent ESR investigations on the triplet state of the primary donor in *Rps. viridis* indicate that in this state the unpaired electrons are also asymmetrically distributed over the two dimer halves [36,37]. In the light of these findings it might appear necessary to reexamine the assignments of the hfcs in the BChl **a** dimer cation radical $P_{870}^{+\cdot}$ [13–16] with possible consequences for the symmetry of the spin distribution in this species.

It is interesting that in plant photosystems 1 and 2 the ESR spectra of the respective oxidized electron donors ($P_{700}^{+\cdot}$ and $P_{680}^{+\cdot}$) show a linewidth similar to that of oxidized monomeric chlorophyll **a** (Chl $\mathbf{a}^{+\cdot}$) [3,28,38,39]. Consequently, monomeric Chl **a** species have already been proposed for $P_{680}^{+\cdot}$ [38] and for $P_{700}^{+\cdot}$ [40]. An asymmetric dimer with the unpaired electron located mainly on one half could equally well explain the observed ESR and ENDOR spectra [28,45] [#1].

The asymmetrical spin density distribution of the donor P in its oxidized state could be an essential requirement for the high efficiency of the primary charge separation $PI \rightarrow P^+I^-$ (I: intermediate acceptor bacteriopheophytin) in the photosynthetic reaction center. It is evident that the back-reaction would be effectively impeded if the unpaired electron (or positive hole) in $P^{+\cdot}$ retreats to that side of the dimer which is more remote from the acceptor I on the photoactive branch or from some intermediate species acting as a spacer. Similarly, the efficiency of the forward reaction would gain by an asymmetrical orbital charge distribution of the "excited" electron in the state $^1P^*$ in favor of the *other* dimer half facing the photoactive branch [46]. Calculations of the spin density distribution of the donor *anion* radical $P_{960}^{-\cdot}$ in which the unpaired electron occupies the same orbital as the excited electron in $^1P^*$ do, in fact, show a reversal or "switch behavior" of orbital charge distributions between the dimeric halves of the donor [21]. These results point to a charge separation *within* the dimer upon singlet excitation which is supported by the strong Stark effect experienced by the dimer band in the optical spectrum [47,48]. Details of our theoretical investigations will be published in a forthcoming paper [31].

[#1] It should be noted that monomers or dimers of *structurally different* chlorophylls [41–44] have also been proposed to form the primary donor in photosystem 1.

Acknowledgement

The authors thank S. Schroy and C. Bubenzer (Munich) for their expert technical assistance in preparing the reaction centers. We are grateful to H. Michel (Max-Planck-Institut, Frankfurt/Main) and J. Deisenhofer (H. Hughes Med. Inst., Dallas, Texas) for supplying X-ray coordinates of *Rps. viridis* RCs. Financial help from the Deutsche Forschungsgemeinschaft (Sfb 337 and 312 in Berlin, Sfb 143 in Munich) and the Fonds der Chemischen Industrie (WL) is gratefully acknowledged. Work done in Leyden (AJH) was supported by the Netherlands Foundation for Chemical Research (SON) financed by the Netherlands Organisation for Scientific Research (NWO).

References

[1] A.J. Hoff, Phys. Rept. 54 (1979) 75.
[2] M.Y. Okamura, G. Feher and N. Nelon, in: Photosynthesis: energy conversion by plants and bacteria, Vol. 1, ed. Govindjee (Academic Press, New York, 1982) p. 195.
[3] F.K. Fong, ed., Light reaction path of photosynthesis (Springer, Berlin, 1982).
[4] H. Michel, J. Mol. Biol. 158 (1982) 567.
[5] J. Deisenhofer, O. Epp, K. Miki, R. Huber and H. Michel, J. Mol. Biol. 180 (1984) 385.

[6] J. Deisenhofer, O. Epp, K. Miki, R. Huber and H. Michel, Nature 318 (1985) 618.
[7] H. Michel, O. Epp and J. Deisenhofer, EMBO J. 5 (1986) 2445.
[8] K. Möbius, M. Plato and W. Lubitz, Phys. Rept. 87 (1982) 171.
[9] K. Möbius and R. Biehl, in: Multiple electron resonance spectroscopy, eds. M.M. Dorio and J.H. Freed (Plenum Press, New York, 1979) p. 475.
[10] J.R. Norris, R.A. Uphaus, H.L. Crespi and J.J. Katz, Proc. Natl. Acad. Sci. US 68 (1971) 625.
[11] J.R. Norris, H. Scheer and J.J. Katz, Ann. NY Acad. Sci. 244 (1975) 260.
[12] G. Feher, A.J. Hoff, R.A. Isaacson and C.C. Ackerson, Ann. NY Acad. Sci. 244 (1975) 239.
[13] F. Lendzian, W. Lubitz, H. Scheer, C. Bubenser and K. Möbius, J. Am. Chem. Soc. 103 (1981) 4635.
[14] W. Lubitz, F. Lendzian, H. Scheer, J. Gottstein, M. Plato and K. Möbius, Proc. Natl. Acad. Sci. US 81 (1984) 1401.
[15] W. Lubitz, F. Lendzian, H. Scheer, M. Plato and K. Möbius, in: Photochemistry and Photobiology, Proceedings of the International Conference, University of Alexandria, Egypt, ed. A.H. Zewail (Harwood, New York, 1983) p. 1057.
[16] W. Lubitz, R.A. Isaacson, E.C. Abresch and G. Feher, Proc. Natl. Acad. Sci. US 81 (1984) 7792.
[17] M.S. Davis, A. Forman, L.K. Hanson, J.P. Thornber and J. Fajer, J. Phys. Chem. 83 (1979) 3325.
[18] F. Lendzian, W. Lubitz, R. Steiner, E. Tränkle, M. Plato, H. Scheer and K. Möbius, Chem. Phys. Letters 126 (1986) 290.
[19] M. Plato, E. Tränkle, W. Lubitz, F. Lendzian and K. Möbius, Chem. Phys. 107 (1986) 185.
[20] W. Lubitz, F. Lendzian, M. Plato, E. Tränkle and K. Möbius, in: Proceedings of the XXIII Congress Ampere on Magnetic Resonance, Rome 1986, p. 486.
[21] M. Plato, F. Lendzian, W. Lubitz, E. Tränkle and K. Möbius, Proceedings of the Nato Workshop "Structure of the Photosynthetic Bacterial Reaction Center", Cadarache, France, 1987 (Plenum Press, New York), to be published.
[22] G. Jolchine and F. Reiss-Husson, FEBS Letters 40 1974) 5.
[23] J.M. Pachence, P.L. Dutton and J.K. Blasie, Biochim. Biophys. Acta 548 (1979) 348.
[24] P.W. Holloway, Anal. Biochem. 53 (1973) 304.
[25] H.J. den Blanken and A.J. Hoff, Biochim. Biophys. Acta 681 (1982) 365.
[26] R. Steiner, E. Cmiel and H. Scheer, Z. Naturforsch. 38c (1983) 748.
[27] E. Cmiel, S. Schneider and H. Scheer, to be published.
[28] F. Lendzian, Ph. D. Thesis, Freie Unversität Berlin, Berlin (1982).
[29] M.J.S. Dewar, J.A. Hashmall and C.G. Venier, J. Am. Chem. Soc. 90 (1968) 1953.
[30] J.A. Pople and D.L. Beveridge, Approximate molecular orbital theory (McGraw-Hill, New York, 1970).
[31] M. Plato, F. Lendzian, W. Lubitz, E. Tränkle and K. Möbius, Israel J. Chem. (1988), to be published.
[32] W. Lubitz, F. Lendzian, M. Plato, H. Scheer and K. Möbius, in preparation.
[33] R.C. Dougherty, H.L. Crespi, H. Strain and J.J. Katz, J. Am. Chem. Soc. 88 (1966) 2854.
[34] J.J. Katz, R.C. Dougherty, H.L. Crespi and H. Strain, J. Am. Chem. Soc. 88 (1966) 2856.
[35] J.S. Hyde, G.H. Rist and L.E. Erikkson, J. Phys. Chem. 72 (1968) 4269.
[36] J.R. Norris, C.P. Lin and D.E. Budil, J. Chem. Soc. Faraday Trans. II 83 (1987) 13.
[37] E.J. Lous and A.J. Hoff, Proc. Natl. Acad. Sci. US 84 (1987) 6147.
[38] M.S. Davis, A. Forman and J. Fajer, Proc. Natl. Acad. Sci. US 76 (1979) 4170.
[39] M.R. Wasielewski, J.R. Norris, H.L. Crespi and J. Harper, J. Am. Chem. Soc. 103 (1981) 7664.
[40] P.J. O'Malley and G.T. Babcock, Proc. Natl. Acad. Sci. US 81 (1984) 1098.
[41] M.R. Wasielewski, J.R. Norris, L.L. Shipman, C.P. Lin and W.A. Svec, Proc. Natl. Acad. Sci. US 78 (1981) 2957.
[42] H. Scheer, E. Gross, B. Nitsche, E. Cmiel, S. Schneider, W. Schäfer, H.-M. Schiebel and H.-R. Schulten, Photochem. Photobiol. 43 (1986) 559.
[43] D. Dörnemann and H. Senger, Photochem. Photobiol. 43 (1986) 573.
[44] T. Watanabe, M. Kobayashi, M. Nakazato, I. Ikegami and T. Hiyama, in: Progress in photosynthesis research, Vol. 1, ed. J. Biggens (Nijhoff, Dordrecht, 1987) p. 303.
[45] K. Möbius and W. Lubitz, in: Biological magnetic resonance, Vol. 7, eds. L. Berliner and J. Reuben (Plenum Press, New York, 1987) p. 190.
[46] M.E. Michel-Beyerle, M. Plato, J. Deisenhofer, H. Michel, M. Bixon and J. Jortner, Biochim. Biophys. Acta 932 (1988) 52.
[47] M. Lösche, G. Feher and M.Y. Okamura, Proc. Natl. Acad. Sci. US 84 (1987) 7537.
[48] D.J. Lockhart and S.G. Boxer, Proc. Natl. Acad. Sci. US 85 (1988) 107.